Journal of Robotics and Control (JRC)
Volume 5, Issue 5, 2024
ISSN: 2715-5072, DOI: 10.18196/jrc.v5i5.22558

Predicting SI Engine Performance Using Deep Learning with CNNs on Time-Series Data

Mohamed S. Hofny [1], Nouby M. Ghazaly [2], Ahmed N. Shmroukh [3], Mostafa Abouelsoud [4]
[1, 2, 3, 4] Department of Mechanical Engineering, Faculty of Engineering, South Valley University, Qena 83523, Egypt
[2] Technical College, Imam Ja'afar Al-Sadiq University, Baghdad, Iraq
[3] Faculty of Industry and Energy Technology, New Cairo Technological University, Cairo 11835, Egypt
Email: [1] Mohamed.Salah@eng.svu.edu.eg, [2] Nouby.Ghazaly@eng.svu.edu.eg, [3] ahmed.shmroukh@eng.svu.edu.eg, [4] mostafa.soud@eng.svu.edu.eg
*Corresponding Author

***Abstract*—In this study, deep learning (DL) model is used to predict brake power (BP) of GX35-OHC 4-stroke, air-cooled, single-cylinder gasoline engine. The engine uses E15 (85% gasoline + 15% ethanol) as a fuel due to its high performance and low emissions. A convolutional neural networks (CNN) model is used on time-series data due to their ability to capture temporal patterns and relationships in sequential data, such as engine BP. While studying the performance of the network, it is found that the root mean squared error (RMSE) is 0.0007, explained variance score (EVS) is 0.9999, and mean absolute percentage error (MAPE) is 0.22%. Compared to traditional machine leaning methods, these metrics demonstrate the high accuracy and reliability of the model, confirming its effectiveness in predicting BP. Various performance curves are plotted such as comparing target and predicted values, regression plots (to indicate the generalization capability), learning curve (to demonstrate the model's effective training progress and convergence), Bland-Altman plot (to show the convergence between the actual and predicted values), histogram and density plot (to show a close fit between predicted and actual values), density plot of actual and predicted outputs, and residual plot (to show randomly distributed errors). This high accuracy and reliability of this DL model help in effective real-time engine performance monitoring, and reducing emission levels, especially for the adoption and use of renewable fuels like E15.**

Keywords—Deep Learning; Convolutional Neural Network (CNN); Engine Performance; SI Engine.

I. INTRODUCTION

Internal combustion (IC) engines, which include both compression ignition (CI) and spark ignition (SI) engines are widely used in various applications such as automobiles and trucks [1]. CI engines also known as diesel engines, ignite fuel through the heat produced when air is compressed [2], while SI engines, also known as gasoline engines, make use of spark plug to ignite the air-fuel mixture [3]. These engines are preferred due to its high power density, they operate with high performance through various speed range [4][5][6]. The development of IC engines has become very rapid, focusing on enhancing engine performance and reducing emissions [7][8][9]. The development of SI engines has been known with replacing gasoline with natural gas or blending various alternative fuels with gasoline [10][11][12]. Recently, ethanol-gasoline blends have become very common fuel as it produces high performance and low emissions [13][14].

There are different studies showed the use of machine learning (ML) techniques in IC engines to improve the prediction of performance and emissions such as decision tree (DT) [15], support vector regression (SVR) [16], random forest (RF) [17], gradient boosting machines (GBM) [18], artificial neural network (ANN), and response surface methodology (RSM) [19][20]. ANNs are one of the most prominent techniques used to predict ICE [21][22][23]. These models have been used to forecast engine performance metrics such as torque, combustion chamber pressure, exhaust gas physical qualities, and vibration. Additionally, ANN has been used for defect detection, misfire diagnostics, and combustion timing management in IC engines [19][24][25][26]. Also, support vector machines SVMs are powerful mathematical tools used for classification, regression, and function estimation [27][28]. It is observed that the SVM model is a powerful method in predicting engine performance and emissions because they provide a high accuracy [29]. These previous studies using traditional ML techniques have not achieved the highest accuracy in predicting engine performance and emissions in real-time.

Deep learning (DL) that is considered a sub-branch of ML algorisms, depends on identifying various layers of distributed representations. At last years, deep learning is used in various applications for classic problems [30].Top of Form DL algorithms are able to enhance ML algorithms with advanced models that has various layers of processing to enable the learning of data representation through different levels of abstraction. This field causes significant advances in various field's performance such as speech and visual object recognition, object detection, and areas like drug discovery and genomics. With using backpropagation algorithm, deep learning added complex patterns with extensive datasets and guided the machine to adjust its internal parameters. These adjustments help compute the data representation in one layer based on the information from the preceding layer [31]. DL techniques can be used for linear regression analyses on datasets. Generally, when applying a model on a small sample, one of the major things to consider is the case of over fitting. These are concerns using the present model Definition Adjusting the model's parameters to reduce these concerns [32]. These methods open up good research opportunities for studying the performance characteristics of SI engines, to enable better

fuel economy and, at the same time, impacting on the operational costs. Hence, the objective of this study is to improve the prediction accuracy of engine performance (BP) via CNN, and offer real-time and accurate data to broaden the range of engine management.

Deep learning is a current machine learning approach used to design complex neural networks with multiple layers of neurons to map and learn the complexity in big data set [33]. Some of these networks have provided new state of the art solutions for a number of problems. This has made DL algorithms in ANN capable of handling complex information as a result of the complexity of the algorithms. However, the investigated networks and the mechanism underlying them involve a feature that allows them to learned data representations at multiple hierarchal levels [31]. There has been significant improvement for deep neural networks in the last years. But their performance in supervised learning tasks depends on the availability of a large volume of training data. In an attempt to overcome this, ways of data enhancement have been developed to increase the sizes of the training data artificially [34].

Several real-world applications have been solved efficiently using Deep learning (DL) techniques, thus Pioneering its use in many conditions monitoring (CM) studies. While these studies present a high success rate in identifying DL architectures for various applications, there is a lack of comprehensive recommendations on choosing the right architecture and its relevance achieved through feature learning in such research [35]. These can learn features from the raw data and have been found to be very useful in recent times in many fields. It can be attributed to the increase in computational capabilities, availability of cloud computing, the creation of new and convenient analytical tools and frameworks and enormous datasets [36], [37]. With the amount of data rising, the DL method features high performance during the testing stage, even though the training phases might be very long. A critical feature in making DL efficient is reliance on assorted matrix computations; therefore, DL lends itself well to GPU processing [38]. Top of FormTop of Form Convolutional Neural Networks (CNNs) have become an important field of study since the introduction of the basic CNNs in 1990 and they are widely used today as the default architectures in different machine learning and computer vision tasks. In which the 2012 ILSVRC contributed in creating a significant impression, showing that deep CNNs are very much capable to perform well and efficiently on image classifications. One of the key drivers of the popularity of deep CNNs has been tremendous improvements in the processing capability of computers that are available in the market today [39]. Generally, CNNs are a type of feed-forward neural networks that feature alternating layers of convolution and subsampling, and they are primarily trained using supervised learning methods [40].

Deep learning has been used In adsorption properties of metal−organic frameworks to construct accurate models for quantitative structure-property relationships (QSPR) that quickly forecast the working capacity of CO2 and the selectivity of CO2/N2 under low-pressure scenarios pertinent to post-combustion carbon capture (0.15 bar CO2, 0.85 bar N2) [41]. Ağbulut et al. used DL algorithm to predict brake specific fuel consumption (BSFC), brake thermal efficiency (BTE), exhaust gas temperature (EGT), CO, and NOx emissions It is evidenced that DL algorithms prove to be very efficient of estimating the performance and emission of CI engines and can be employed for real-time engine monitoring and improvement [42]. Shin et al. proposed a model based on deep neural networks for the prediction of several aspects related to common gasoline engine efficiency. This model is divided into two sub-models: the first is an approach that can be used for predictions on cases such as engine knock while the second covers prediction of factors like engine performance, combustion features, and emission rates. They used an advanced DL algorithms to predict multiple engine outputs simultaneously, including emissions and performance indices like BSFC and brake-specific nitrogen oxides (BSNOx). These models consistently achieved high R^2 values (above 0.99) and low RMSE, indicating high predictive accuracy [43]. Lee et al. employed the deep learning approach to forecast the dynamic characteristic of design parameters of diesel engine valve train. Of all the models that were tried, it was observed that the one-dimensional convolutional neural network (1D-CNN) had the best results. The 1D-CNN increased the prediction accuracy for valve train force and valve seating velocity which are important for efficiency and life cycle of the engine [44]. Papagiannakis et al. used DL in improving the prediction of the engine performance and emissions in the study. Particularly, the 1D-CNN model provided higher accuracy in terms of predicting valve train force and valve seating velocity having the R2 Scores of 0.89 and 0.98 respectively. This implies that deep learning models especially the 1D-CNN could enhance the forecasting of critical parameters of the engine hence enhancing the engine performance and its lifespan [4]. Pulvirenti et al. employed a similar DL model for estimating the vehicle speed and explained how the incorporation of the prediction as a component of energy management is superior to the powertrain control approach. A new Adaptation algorithm is proposed that uses the speed prediction to improve an A-V2X-ECMS. This approach makes use of the driving pattern recognition to modify the equivalence factor of the ECMS in the event that there are changes in some driving patterns or SoC significantly departs from its desired value [45].

Cantero-Chinchilla et al. have made a study on ultrasound corrosion profile time series regression, a proposed customized convolutional neural network (CNN) architecture is presented for estimating the thickness values (minimum and mean) of corroded profiles from ultrasonic time-series measurements (A-scan). The architecture of the CNN is determined by the optimization of the hyper-parameters that identifies the most effective network performance [46]. Dou et al. have constructed a DL model to develop a lightweight diagnostic method using thermal parameters to indicate the importance of these parameters in IC engines diagnosis. Deep learning capability in this approach plays a role in analyzing and interpreting thermal data as a different approach to diagnosing engine health and status [47]. Using the same DL model, Vellandi et al. have attempted at identifying the depth of surface mixture that

can be collected using a handheld microscope from given RGB images. This could assist in demonstrating the capability of DL in elucidating visual information and support profound texture depth examination without having the need for wanton and costly operative instruments [48]. Tajima et al. have done a work that consists of the use of deep learning processes to forecast instances of engine knock using past records in the form of in-cylinder pressure data gathered from experiments. This was done to identify the most critical period within the pressure history for accurate knock prediction. Supervised deep learning techniques were applied, using the in-cylinder pressure history as input and labeling each cycle based on the presence or absence of knock. To address the challenge posed by the imbalance between knock and non-knock cycles, the learning process was conducted both with and without cost-sensitive approaches, to assess their impact on prediction accuracy [49]. Rana et al. have been modeled a CNN for the multi-step ahead prediction of thermal solar collectors' generation in addition to the immediate time horizon. This technique has also been used in the prediction of thermal energy utilizing solar power within a building cooling system as part of a central controller's forecasting system [50]. These are involved challenges like the exhaust emission control and the enhancement of fuel economy. In this way, applying DL capabilities, we can improve the accuracy of the models for monitoring the engine processes and escalating the performance. This in the long-run helps to bring about better and efficient engine performance.

The deployment of machine learning as a technique of predicting the transient emission characteristics of diesel engines has the following advantages; faster computation time, these techniques consume less resources and have a high forecasting accuracy and are generally more reliable [51]. Over the past few years, deep learning methodologies have been identified as a relevant area of study for RUL prediction. Such advance methods have been acknowledged for improving the accuracy and reliability of the prognostic predictions [52]. There has been a sharp increase in research activity related to time series forecasting; the rate at which studies are conducted on this has even quickened in the recent past. It outlined that deep neural networks have become stable tools likely to achieve reliable performance in very many applications. Consequently, less these networks have become one of contemporary's most frequently utilized approaches to solving the challenges of big data [53]. This work is to utilize time-series data prediction using CNNs to explore the deep learning in predicting the engine performance and emissions from SI engines. The usage of CNNs is beneficial due to the large amount of data it handles and the way it extracts the features through layers, hence, making it preferable to traditional models of machine learning that are dependent on feature extraction. The aim is to increase the efficiency and precision of forecast pertaining to the engine output and emissions; in other words, to provide realistic time available for comprehensive engine control and contribution to environmental policies. However, there is still a gap especially in the use of the DL for prediction of the SI engine power utilizing the time series data. Thus, this contribution fills the gap in the literature through the integration of CNNs that can handle big data and perform extraction through layers while surpassing basic ML models. Its aim is to enhance reliability of the estimation of the engine performance (BP) qualified in real-time control of the engine and demonstrate the effectiveness of CNNs in predicting IC engine performance.

II. METHOD

A. Test-Rig Installation

The experimental engine employed in the study was a GX35-OHC 4-stroke, air-cooled, single-cylinder gasoline engine of details summarized in Table I from the manufacturers as depicted in Fig. 1. The following table presents all the parts involved in the study. The dynamometer was an HM-365 and the engine was placed in a CT-159 unit that comprises of several measuring devices like the temperature and flow sensors. For CNN experiments, the procedure commenced by channeling air through a blower as indicated in Fig. 2. This blower introduces fresh air into a conduit, leading it through a flow control valve used to adjust airflow and into an electric air heater that elevates the temperature (this temperature was measured but not controlled by the air temperature sensor in CT-159 unit). Following this, the air traverses a filter and flowmeter, which gauges air consumption in liters per minute. The air proceeds to the carburetor, mixing with a specified quantity of E15 fuel before it enters the engine's combustion chamber. Simultaneously, the fuel level in the fuel measurement tube decreases, a change that can be directly observed or calculated via a connected computer so, fuel consumption also was measured not controlled. Engine speed was controlled by speed control wire on CT-159 unit. Engine torque was controlled by HM-365 unit. Engine parameters are observed through external computer. These previous steps are shown in Fig. 3.

TABLE I. ENGINE SPECIFICATIONS USED IN EXPERIMENT [57]

Engine Type	4-stroke single cylinder air cooled OHC petrol engine
Bore X Stroke (mm)	39 x 30 mm
Compression ratio	8.0: 1
Ignition System	Transistorized
Net Power	1.0 kW (1.3 HP) / 7000 rpm
Oil Capacity	0.1 Liter
Starting System	Recoil
Displacement	35.8 cm3
Fuel cons. at cont. rated power	0.71 L/h - 7000 rpm
Max. net torque	1.6 Nm/ 5500 rpm
Idle speed	2800RPM
Lubrication	Oil mist
Carburetor	Ruixing Brand Carburetor

In this study, BP is taken to be studied. The load was operated under both constant and varying loads, the load was constant to study the engine performance due to other input parameters and then it was varied to study its effect. series of measurements are taken to assess a set of experimental parameters, designated by "n". This aggregate of observations is then utilized to ascertain the central experimental result. Consequently, eq (1) can be employed to calculate the average value of the quantities recorded during the experiments [54]. The variable X_m corresponds to

the observed value, and the variable n signifies the total number of observations made. Eq (2) describes the method for deriving the standard deviation (SD), and eq (3) provides the calculation for the uncertainty (U) as indicated in Table II [55][56]. The duration of the experiment was selected so that the engine achieved a stabilized operating mode and a sufficient number of samples was obtained to characterize the operational characteristics and emissions with one data point per ten seconds under variable and constant load. Values that were missing were interpolated using cubic spline since this helps in generating values that are quite close to the real values. Interquartile range or IQR was used to deal with the outliers either by eliminating them or restricting them in order to avoid distorting the training of the model.

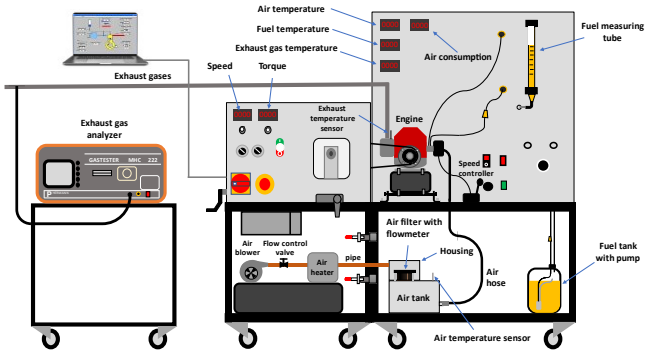

Fig. 1. Experimental test rig

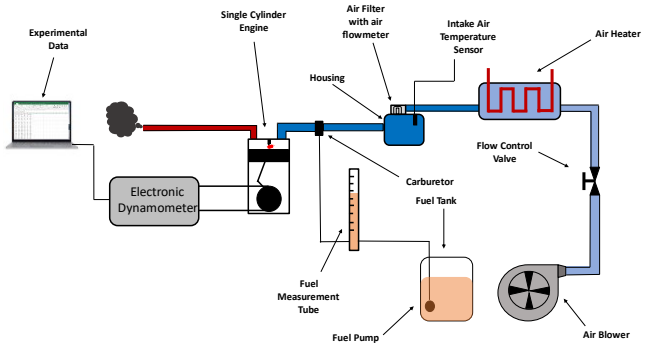

Fig. 2. Experimental installation cycle for CNN

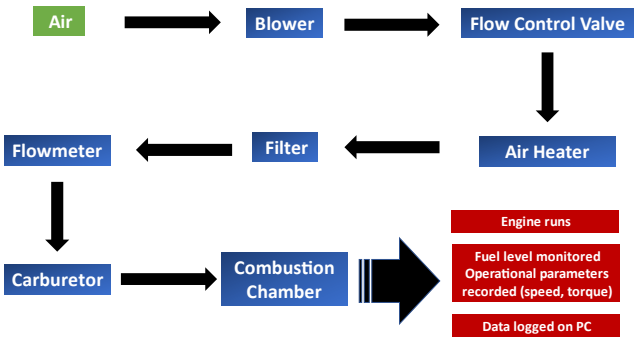

Fig. 3. Flowchart of experimental procedure

TABLE II. UNCERTAINTY MEASUREMENTS

Measurement	Uncertainties
Load	± 0.01 N
Speed	± 10 rpm
Temperature	± 1°C
BP	±1.60

$$\bar{X} = \frac{\sum Xm}{n} \quad (1)$$

$$SD = \sqrt{\frac{\sum_{m=1}^{n}(Xm-\bar{X})^2}{(n-1)}} \quad (2)$$

$$U = \frac{SD}{\sqrt{n}} \quad (3)$$

B. *Architecture of CNNS*

In our study, a CNN deep learning model shown in Fig. 4 is used to predict BP. The input shape is a structured array or tensor that includes various operational parameters of an engine, such as engine speed, engine torque, air temperature, air flowrate, and fuel consumption. Each input vector to the same instance in time, to form a snapshot of the engine's operational state. This input is what the network will use to predict the subsequent outputs related to engine performance and emissions. Convolutional layers (Conv1D) are designed to progressively reduce the dimensionality of the feature maps while preserving essential information. That involve the application of filters to the input to create feature maps. These maps themselves differ in that they may contain key characteristics of the data, such as patterns or trends that the network can use [58]. After each Convolution layer there is Max pooling layer (MaxPooling1D) to reduce the dimensions of the feature maps in order to make the feature representations invariant and also to reduce the computational time. It helps in avoiding overfitting in the model since it lowers the total count of parameters in the model [59]. Max pooling achieves this by taking the maximum value over a window of specified size (the pool size) and stride over the feature map. This operation retains the most significant elements of the feature maps, ensuring that the network remains sensitive to the most prominent features while gaining a degree of translational invariance [60]. Together, these convolutional and pooling layers form the feature extraction part of the CNN, which is critical for learning task-specific features directly from the data without the need for manual feature engineering.

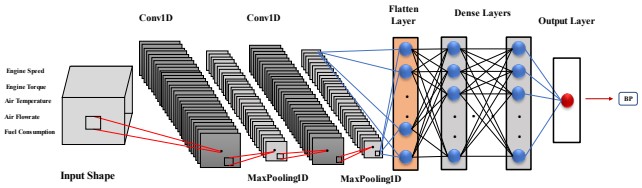

Fig. 4. Architecture of CNN

The flatten layer is the point where the multi-dimensional output from the preceding max-pooling layers is transformed into a one-dimensional vector. This is necessary because the following dense layers, which are also referred to as fully connected layers, require a fixed-length input vector. After the input data has gone through convolutional and pooling layers which are designed to process and condense the information, the high-level features that have been extracted are laid out in a long vector through the flattening process [61]. The flatten layer does not learn any parameters; instead, it is a simple data restructuring step. If the output of the preceding max-pooling layers is a multi-dimensional array (for example, a

3D array with dimensions corresponding to the number of feature maps, height, and width), the flatten layer takes this array and converts it into a 1D array by laying out each of the elements in a single long sequence. This 1D array is then fed into the dense layers for further processing, which typically involves learning the final high-level features and performing classification tasks [62]. The dense layers combine these features in various ways, learn during training which features are important for the task at hand, and ultimately produce the predictions at the output layer.

The dense layers are a series of layers that come after the flatten layer. These layers are called "dense" because every neuron in each dense layer is connected to every neuron in the preceding layer, which is not the case in convolutional layers where neurons are only connected to a small, localized region of the previous layer [63]. The flattened output serves as the input to the first dense layer. Each neuron in these dense layers will perform a weighted sum of the inputs, apply a bias, and then usually pass the result through a non-linear activation function. The purpose of the dense layers is to interpret the features extracted by the convolutional and pooling layers in order to make a final prediction. The dense layers are where the CNN starts to make sense of the information that has been distilled by the convolutional and pooling layers [64]. They are capable of modeling complex functions because of the high level of interconnectivity between neurons. In your diagram, you can see two dense layers, each followed by an activation function (not specifically shown, but typically implied between layers in such diagrams) [64]. The last dense layer is connected to the output layer. This final layer is tailored to the specific task the network is designed to perform [65]. For example, in classification tasks, the output layer often has as many neurons as there are classes, and a softmax activation function is typically used to produce a probability distribution over the classes.

The output layer has one neuron that comes from the preceding dense layer. The dense layer neurons will process the features from the entire network and pass their weighted outputs to the neuron in the output layer [66]. The activation function used in the output layer depends on the type of prediction the network is performing. For regression tasks, the output layer might use a linear activation function. The final output of this neurons is typically a set of values that are interpreted as the prediction of the network. In a regression task, these values might directly represent the predicted quantities [67], [68].

C. Prediction of Brake Power

The implemented CNN is designed for the regression of time-series. Prior to model input, features undergo normalization through Minmax scaling, adjusted to a [0, 1] range, excluding the target feature 'Brake power', which is scaled independently. This scaling is used because it reduces the time it takes for the model to converge, increases the numerical stability and improves the efficiency of the gradient descents [69]. The architecture processes sequences of 30 consecutive data points to reflect the inherent temporal structure of time-series data. This selection as the short intervals of the engine operation contains distinct temporal patterns in performance data. This selection considers the context acquisition alongside the computational complexity, and previous work indicates that it suffices for effective modeling in such tasks [70]. The dataset is divided into training (70%, further subdivided into training and validation subsets), validation (15%), and testing (15%) segments to facilitate comprehensive training and evaluation. This splitting strategy makes sure that the model is trained deeply, as well as validated is to avoid overfitting of the data and tested to be sure that it is not overfitted and that it can generalize well to new data [14].

Initially, the CNN is configured with default settings. The input layer is designed to accept sequences shaped (30, number of features), where the dimensionality depends on the specific dataset used. The first convolutional layer consists of 64 filters with a kernel size of 3 as it is effective in capturing local temporal patterns in the time-series data [71], utilizing the ReLU activation function to introduce non-linearity ensuring that the model can efficiently and effectively learn from the complex time-series datamin [72], while the second convolutional layer includes 128 filters, also with a kernel size of 3 and ReLU activation. The selection of filters 64 and 128 was performed taking into account the fact that these values would be able to capture some features of the input data and gave high performance network. The first convolution layer with the 64 filters extracts simple patterns of data and the second convolution layer with 128 filters extracts more high-level features of the data so as to make the model strong enough to learn more features of the data fed to it [73]. Each convolutional layer is succeeded by a max pooling layer with a pool size of 2, aimed at reducing spatial dimensions and enhancing feature extraction. The flattening layer converts the multidimensional output of the previous layers into a 1D feature vector. The dense layers comprise a series of fully connected layers with decreasing units from 50 to 10, employing ReLU activation, and culminate in a single-unit output layer with linear activation to predict the scaled 'BP'.

The model is compiled using the Adam optimizer due to its self-adjusting functionality that maintains and improves convergence rates for the parameters speeding up and increasing the viability of the training process in large datasets. The learning rate is 0.001 to minimize the mean squared error (MSE) loss function and ensure steady convergence. It is trained over 100 epochs for training without getting overfitted, further helped by early stopping according to the validation accuracy obtained. The batch size is 32 so that more precise gradient was obtained during the training phase, with close monitoring of validation performance. This process helped avoid overfitting to some degree since the model’s general structure was validated using K-fold cross validation tests; the dropout layers were implemented with a probability of 0. 5 drop out rate and L2 regularization to make sure that the system does not over-fit the text data. Another regularization technique that was used was early stopping given that training was stopped when the validation loss did not decrease in some predefined epochs. These techniques in combination with the evaluation metrics like RMSE: RMSE, EVS, and MAPE all make the CNN model more reliable and robust. All the training and

evaluation of the CNN model were conducted in a 12 th Gen Intel (R) Core (TM) i7-12700H processor with 14 cores CPU and 20 logical processors, Nvidia Geforce RTX 3060 graphic card, 16GB RAM and SSD as storage media. For implementation, TensorFlow was used; Python was used, along with NumPy, pandas, scikit-learn, and matplotlib. The average computational time was around 5 minutes. The information regarding the hardware infrastructure and computational time enables one to assess the feasibility of the practical application of this model.

After training, the model's effectiveness is assessed on the test set using metrics such as Root Mean Squared Error (RMSE), Explained Variance Score (EVS), and Mean Absolute Percentage Error (MAPE). These metrics are selected in order to arrive at a realistic evaluation of the given model's performance. The purpose of RMSE is to indicate the average size of errors, which concerns the accuracy of the model. EVS provides the percentage of variation that is explained to the samples that signify the performance of the model in explaining the variability in data. MAPE presents a normalized measure of the accuracy of predictions as to the size of the errors and their comparison. Combined, all these measures facilitate an exhaustive assessment of the model's ability to predict. There are some limitations of the experiment and the used CNN model that we would like to mention. Some of the limitations in experiments include, limited data to be used when trying to generalize the results, and changes in environment may affect the continuity of the experiment. The limitations faced by the by the CNN model included sensitivity to hyperparameters and the large amount of time and resources needed to train the model. The outline of the flowchart starting from data collection right down to result analysis is pointed out in Fig. 5.

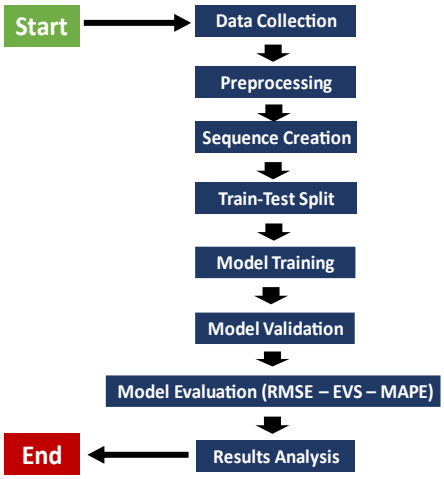

Fig. 5. Flowchart evaluation for CNN model

III. Results and Discussion

A. Performance Metrics

Various performance metrics such as RMSE, EVS, and MAPE are evaluated to test the performance of the model. It is found that RMSE is 0.0007, EVS is 0.9999, and MAPE is 0.22%. Moreover, for the features considered in the research, the Pearson correlation coefficients (Pearson's r) of the model based on the training, validation, and testing datasets all equal 0. 9999. These all-previous metrics give an indication of high accuracy and reliability in predicting BP. Concerning the prediction accuracy measures, a low RMSE reveals that there are fewer prediction errors, EVS is high meaning that the model accounts for most of the disturbances in the data and MAPE is also low revealing that the percentage error is small. Higher values for Pearson's r also affirm the presence of a strong positive linear relationship between the actual performance level and the level predicted by the model, thus establishing that the present model accurately recreates the pattern(s) that define engine performance. The regularly high performance of the developed model on various datasets also suggests good generalization ability on unseen data and the ability of the model to make accurate predictions.

The validation and testing sets are briefly discussed to show that the model performs well on new data; however, more explanation is needed to prove the reliability of the CNN model's prediction Further details include a 70%:15%:15% split to create training, validation, and testing sets While using splitting ratios, K-fold cross-validation was applied to ensure that the results from the split datasets are unbiased is obtained by partitioning the data into. From Table III, it can be deduced that the proposed model has good predictive and generalization capability. These procedures also give confidence on the aspects of generalization and reproducibility of the formulated model, implying its practical utility.

TABLE III. Cross Validation Results

Metric	Values
RMSE	0.0022, 0.0020, 0.0015, 0.0017, 0.0017
Average RMSE	**0.0018**
EVS	0.9996, 0.9996, 0.9995, 0.9998, 0.9994
Average EVS	**0.9996**
MAPE	0.71%, 0.63%, 0.36%, 0.65%, 0.44%
Average MAPE	**0.56%**

There is the tendency of overfitting especially with the high training accuracy demonstrated here. In order to minimize overfitting and to achieve higher accuracy for unseen data, the following types of the regularization were applied. Dropout layers with the dropout of 0. 5 when training was used to randomly eliminating some neurons in order to avoid over dependence on some neurons during training of the model. Besides, L2 regularization was used to prevent the weights from being too large, which can be helpful to achieve small generalizable weights. Another regularization technique applied was early stopping, which stops the training process when the model's performance on the validation set stops improving after a fixed number of epochs. These strategies combined kept the problem in check by ensuring that model complexity did not get out of hand while at the same time increasing the model's capacity to perform well on unseen data.

B. Model Evaluation Plots

1) Comparative Analysis of CNN Predictive Accuracy for Brake Power

Convolutional Neural Network (CNN) model is used for prediction of BP of SI engines using time-series data. Fig. 6.

indicates a high degree of correlation between the predicted and actual values, as shown by the closeness of the data points between actual and predicted data. The y-axis represents BP in (kW), ranging from 0.15 to 0.35 kW and the x-axis represents the sample index, ranging from 0 to 140. Depending on the outcome of the experiment, the following observations can be deduced: from the model, excellent convergence are achieved in the prediction of the values as extracted from the dataset along the range extent as described by the tight distribution of the points along the target variable line. However, certain points of deviation indicate some errors because the stability of engine's operational conditions may be more sensitive to these variable fluctuations, which may not be captured adequately by the model.

It is shown that while the model assesses the profile of fluctuating BP quite well, it occasionally produces numbers that are higher or lower compared to the actual figures. These differences are quite low so, there is a high convergence between actual and predicted values [74]. Therefore, taking into account the data obtained from the analysis of the model being considered, it is possible to declare that there are no tendencies, indicating that the model performs worse on particular samples compared to others. Thus, the results are shown to be satisfactory and accurate [75].

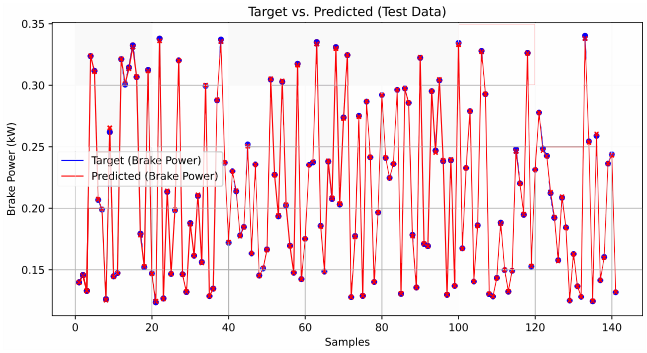

Fig. 6. Target vs. predicted data for the CNN

2) *The Regression Plots for Training, Testing, and Validation Data*

The regression plot for the training data in Fig. 7 shows closely identical results between the model's predictions and the actual outputs. The x-axis indicates the actual output values, ranges from approximately 0.15 to 0.35, while the y-axis represents the predicted output values within the same range. The points are closely clustered around the ideal prediction line, showing that the model has effectively learned the underlying patterns in the training data. This close convergence suggests that the model has been trained effectively. However, it is crucial to examine the potential for overfitting carefully, as high training accuracy does not necessarily ensure strong performance on new, unseen data. The validation data regression plot acts as a tool for assessing how well the constructed model generalizes over the data. As pointed out in the plot of the present study, the prediction from the test set stays rather close to the actual validation, indicating that the parameters of the model have been adjusted well and are not overly trained on the data used in the present analysis.

The testing data regression plot is the last examination of how robust the model in question is. This plot also shows that the model maintains its accuracy even when presented with new values that are never used in training hence it can be applied in real scenarios [76]. This indicates that real-life BP can be fairly predicted using the proposed mathematical model because the calendar time fits quite well with the ideal prediction line. The consistency displayed in all training, validation and testing sets of all the three plots further supports that the CNN model has been trained optimally with little chances of overfitting. The analysis of the model indicates great performance: as we can see from the graphics, the R^2, MSE, and MAE values provide comprehensive evidence of the accuracy and generalization capability of the model. The fact that the CNN had consistent and almost identical numerical results on the three data sets affirms its suitability for the application of predicting BP [77].

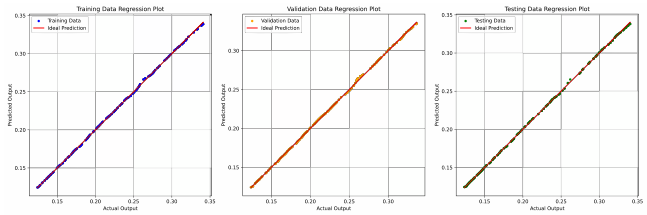

Fig. 7. Regression plots for training, testing, and validation data

3) *Learning Curve for Training and Validation Loss*

Fig. 8 shows the learning curve depicting the performance of loss minimization over epochs for both the training and validation datasets. The y-axis represents the loss, scaled from 0 to 0.25, and the x-axis represents the epoch value, ranging from 0 to 500. The blue line represents the training loss, while the orange line represents the validation loss. Initially, both curves decrease rapidly through few epochs, meaning that the model quickly learns the patterns in the dataset. The convergence between these two curves near zero loss means that the model effectively minimizes loss without overfitting. The overlap here suggests the model complexity is proportional to the data complexity ensuring it will generalize well and perform well on unseen data. This is evident from the high learning rate which implies that the patterns in the data are integrated into the model in the shortest time. The effect is observed at all epochs and shows that the model is not overfitted and can generate an accurate result on new data. The fluctuation of loss closer to zero in subsequent epochs also validates the model's ability to accurately estimate BP. The model implies real activity of learning and is useful for the prediction of real engine performance. Further enhancement of this model, and its application in real world environments, would enable them to forecast on engine performance more accurately.

In this regard, to situate these results within the wider literature, it is necessary to point out that other state-of-the-art models, including basic LSTM and GRU networks, also demonstrate similar trends characterized by a swift

reduction in loss levels and convergence. Nevertheless, it can be seen that the proposed CNN model gives near-zero loss with negligible overfitting which evidence its effectiveness in capturing the temporal relationship in engine performance data. This correlates well with other seal models in terms of predictability and variance of engine performance indicators for which the proposed CNN approach is critical [78], [79].

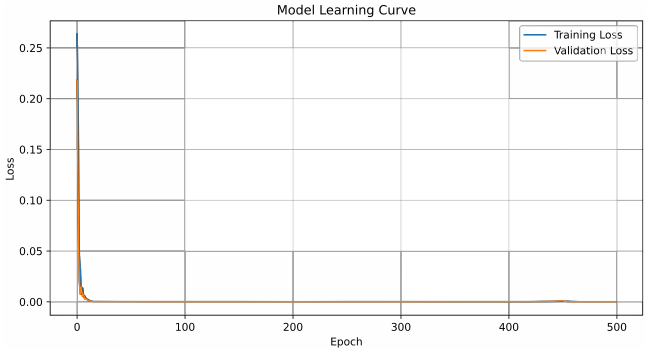

Fig. 8. Learning curve for training and validation loss

4) Bland-Altman Plot

The Bland-Altman plot in Fig. 9 is a critical tool to evaluate the convergence between the CNN model predictions and the actual BP measurements. The plot examines the level of convergence between actual and predicted values. It is worth noting that on the x-axis, there exists the mean of the actual and the predicted values while the y-axis displays their deviations. The red dashed line signifies the mean difference, which is the average bias, closer to zero indicating little or no bias. The blue and green dashed lines represent the upper and lower limits of agreement, showing the range within which, most differences lie, indicating prediction variability. This plot assists in determining systematic bias and accuracy, which most of the points lying inside the limits of agreement it shows that the model has low bias and high accuracy. This plot assists in determining the systematic bias and the level of accuracy with the majority of the points lying within the limits of agreement which show that the model is as accurate as it is unbiased.

The differences shown against the means provide a clear visual representation of the prediction accuracy across the range of measurement. The mean of the actual and predicted values ranges from 0.15 to 0.35, while the differences between the actual and predicted values range from -0.002 to 0.002. The red dashed line indicates the mean difference, which appears to be around 0.000, the blue dashed line represents the upper limit of agreement, set at approximately 0.001, the green dashed line marks the lower limit of agreement, positioned around -0.001. The mean difference, illustrated by the red dashed line, is relatively close to zero, indicating no significant bias in the predictions. The blue dashed lines represent the limits of agreement and it can be noted that most of the predicted values differ from the actual values within a specific range. This means that the variations are normally distributed and can be acceptable. Further, the points are randomly distributed and hence, there is no evidence that the model overestimates or underestimates in certain values.

The Bland-Altman plot presented reveals good agreement between the predicted and the actual values; however, there are some weaknesses. This is due to the nature of the model the presence of outliers and the model does not work as well in certain BP ranges especially 0. 20 to 0. 30 kW. Also, the model may fail for extreme engine conditions which were not encountered during training of the model. These problems therefore suggest the need to accumulate more data and improve on the development of the models to increase the level of accuracy and reliability.

In comparison with the corresponding values in the analyzed literature, the results of the Bland-Altman plot give evidence that the proposed CNN model complies with the high level of accuracy and reliability of real-time monitoring of engine performance [80]. This level of comprehension is comparable to and can be even higher than the comparative conventional machine learning approaches, for instance, SVM and RF. The high level of stably denotes that the current model is rather reliable and mechanically sound to be used in auto or industrial real-world applications [81], [82].

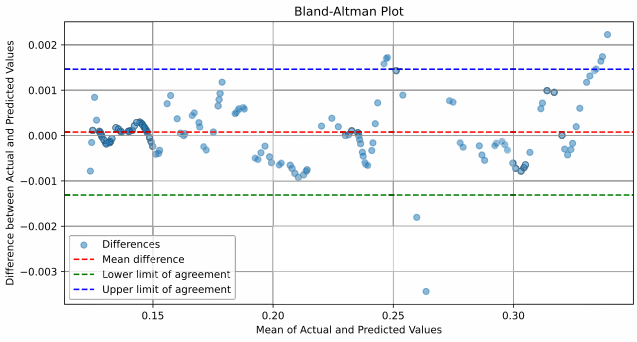

Fig. 9. Bland-Altman plot for actual and predicted values

5) Histogram Analysis of Actual vs. Predicted Brake Power Distributions

The histogram in Fig. 10 shows the distribution of actual and predicted brake power BP values based on the concept of relative frequencies. It can be used in order to achieve the purpose of comparing the distribution of observed and predicted BP data items, and thereby determine alignment and difference. In the blue bars, the actual BP measurements are shown whereas the orange bars illustrate the values from the statistical model. It is noticed that the CNN model's predictions are generally in alignment with the actual values across various ranges of BP. Especially, in the lower range (0.10 to 0.20 kW), the model gives a strong relation between the predicted and actual values, with both sets of data frequently overlapping or being very close to one another.

This shows that the model is very good at this range implying that it can work very well in other ranges of the input data as well. In the middle power: 0.20 to 0.30 kW, some differences are observed, yet there is still relatively much sharing between the groups. Nevertheless, where the BP is greater than 0. 30 kW, the data contains a few outliers that may be improved. These outliers indicate areas where

the prediction model's performance can be better, indicating the necessity of gathering more data in these ranges or improving the modeling methods for managing the extremes. Solving these exceptions is very vital in enhancing the generality and reliability of this model.

In the higher range (greater than 0.30 kW), the model is fairly accurate, though a few outliers indicate potential refinement areas. These variations are small from the overall point of view and the performance of the model is not affected by these but it portrays some indications of where the model is still open for improvements. However, at higher values (greater than 0. 30 kW), the model is still fairly accurate, as predicted values remain close to the actual measurement. However, there are a few cases where predicted values are less than or more than the actual values. These outliers signify regions where model accuracy could be further refined, perhaps by acquiring more data or improving the modeling frameworks [83].

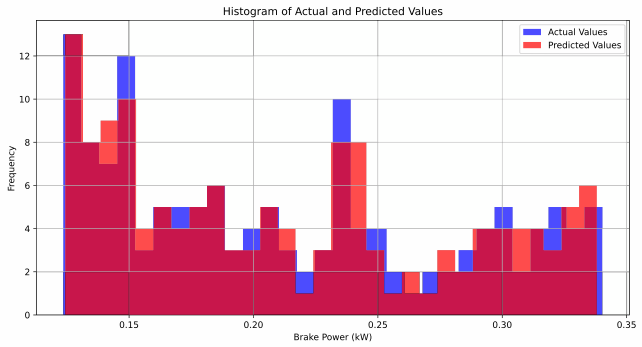

Fig. 10. Histogram analysis of actual and predicted outputs

6) *Density Analysis of Model Predictions Versus Actual Brake Power*

The distribution of the actual and the estimated values of BP through the density plot in Fig. 11. The density plot gives an insight into the probability density of the data, showing how the data is distributed across different values. It provides a better understanding of where the data points are concentrated and how the model performs across the entire range of values. It compares between the actual and predicted value, so, overlapping areas and deviations are more apparent. This is useful for identifying small differences in distribution that might not be as noticeable in a histogram.

Analyzing the graph, it can be seen that there is a good fit between the actual and the predicted therefore proving that the CNN model predicts measures well. This is reflected by the two curves being closely matched at between 0.15 kW, which implies that the accuracy of the prediction system is very high in this range. It is found that there are minor differences between the actual and predicted values at different ranges, especially on the range between 0.25 kW to 0.35 kW, where the predicted values slightly deviate from the actual values. These variations have low values and do not affect the overall performance of the model so, this suggests that while the model performs well.

The general trend of the density plot indicates that the CNN model is reliable across the range of BP values, with consistent predictions that indicates a high convergence with the actual data. There is a smooth and continuous representation of the data distribution, unlike the histogram, which shows the data in discrete columns. This smoothness helps in presenting the overall trend and density of the data more clearly, without the sudden changes that can be seen in a histogram. The overall implications for model accuracy are significant, as regions with high overlap confirm the model's reliability and precision, while areas with deviations highlight the need for additional refinement. Addressing these deviations, possibly through the inclusion of more training data or fine-tuning the model, could enhance the prediction accuracy across the entire BP range.

However, the density plot of the proposed CNN model shows presentable results in comparison to state-of-art models especially in implementing the actual BP dataset [84]. Other models such as LSTM and GRU also demonstrate highly aligned density and likewise high accuracy, however the latter proves CNN's suitability in learning non-linear temporal patterns for a BP range without reduced performance [85]. This works to the advantage of CNN model due to the fact that in situations where precise and accurate engine performance prediction is of essence, then the model is useful.

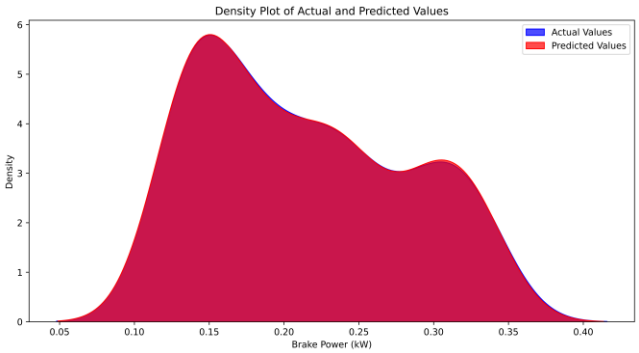

Fig. 11. Density plot of actual and predicted outputs

7) *Residual Analysis for CNN Predictions of Brake Power*

The residual plot displayed in Fig. 12 illustrates the differences between the actual and predicted values of BP, plotted against the sample index. Each red dot represents a residual for a specific data point, with the blue dashed line indicating the zero residual line where the model's predictions would perfectly match the actual values.

The residuals in most frequencies mostly lie within the range of -0.002 to 0.002, which informs that the model has given fairly good estimate values that are relatively close to the true values. This even spread above and below the actual values highlights a well-balanced model performance. Nevertheless, there are a few values that do not fall in this range as shown in the high frequency distribution but it is not prevalent. It is evident that the residuals are symmetrically distributed around the zero line. This symmetry suggests that the CNN model does not exhibit any significant bias in its predictions. The errors are evenly spread above and below the actual values. The residual values could signify that the model's estimates are off by slightly a small range possibly due to similarities in the

training features with those within the calculated residual values.

The information given by the residual plot is important for the assessment of the CNN model's accuracy in estimating BP. The random distribution and random scattering of the residual points around the central line that is equated to zero lead to the conclusion that the model is appropriate and that there are no omitted patterns within the data set. This means that many residuals will be near zero which ultimately emphasizes the high accuracy of the model. However, the remaining plot reveals no clear inconsistency that would indicate a higher level of prediction bias. Thus, a quantitatively deeper error analysis is required to make a diagnosis on the model's robustness. It is significant to report the standard deviation of residuals and investigate the trends in various BP ranges to identify the model's strengths and weaknesses and its validity within the entire population.

The insights derived from the residual plot are also similar to other high-performing approach models used on the analysis of engine performance. Small and mostly randomly distributed residuals and a very narrow range also prove that there are no considerable biases and the CNN model accurately fits the data. Such level of residual analysis is strong evidence of the model's fitness and stability to be utilized for actual implementations where fair and precise anticipations of the engine performance is critical [86], [87].

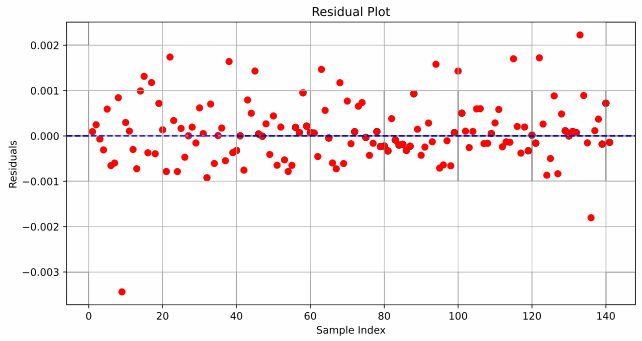

Fig. 12. Residual plot of sample data

C. *Enhancements and Practical Implications of the CNN*

Despite the achieved high predictive accuracy of the CNN model, its further improvements are possible, such as the outliers' handling and boosting the accuracy when predicting BP in precise intervals. Implementing advanced outlier detection and correction techniques, gathering more data, and focusing on the middle power range (0.20 to 0.30 kW) during training could reduce discrepancies. Additionally, employing ensemble learning and hyperparameter optimization may enhance the model's overall robustness and accuracy.

The implications of this research are practical, in that, this study provides information on engine performance monitoring and optimization within IC engine sectors. It enables precise BP predictions and early anomaly detection, and reducing operational costs. The model also can optimize fuel consumption and various emissions, promoting efficiency and environmental sustainability.

IV. CONCLUSION

This study focuses on the application of CNNs for the BP estimation of the IC engines based on time series data. Compared to the feed-forward ANNs, the CNNs can handle big data and can learn features autonomously, thereby improving the performance. The metrics, such as RMSE (0.00007), EVS (0. 9999), and MAPE (0.22%), demonstrate the model's high accuracy in predicting results. Such measures reveal the model's capability to handle nonlinearity and extract temporal features, vital for real-time engine analysis. To avoid overfitting or underfitting of the model, K-fold cross-validation was used to get obtain fair performance estimates, enhancing the dependability and replicability of the results.

Despite achieving good results, it is important to compare these results with other works in the field of engine performance prediction to evaluate their significance. Future studies should explore various architecture of DL such as LSTM networks to learn long-term dependencies and achieve higher predictive capabilities. Additionally, acknowledging several limitations of the study is crucial: the sensitivity of the models to outliers and the performance of the models across different engine types. Looking at these directions in the future work and including different data sets, it is possible to improve the model.

Application of the described approaches can be useful in monitoring the current state and setting new goals for the engine operation, potentially reducing expenses. However, like most machine learning research, the study also has limitations, including the consideration of outliers and generalization to other engine types. Further studies should address less questions while using more datasets, and the utilization of various data types following the outlined model will be useful in the future.

Other application areas include performance enhancement of engine and its monitoring, which can lead to potential decrease of expenses. The study also advances understanding by demonstrating CNNs' applicability in predictive models of IC engines and providing a strong method to improve engine performance analysis. Additionally, different curves and plots were used in analyzing the model and affirming the outcome.

REFERENCES

[1] I. Vinoth Kanna, M. Arulprakasajothi, and S. Eliyas, "A detailed study of IC engines and a novel discussion with comprehensive view of alternative fuels used in petrol and diesel engines," *International Journal of Ambient Energy*, vol. 42, no. 15, pp. 1794–1802, 2021, doi: 10.1080/01430750.2019.1614994.

[2] İ. Temizer, Ö. Cihan, and B. Eskici, "Numerical and experimental investigation of the effect of biodiesel/diesel fuel on combustion characteristics in CI engine," *Fuel*, vol. 270, 2020, doi: 10.1016/j.fuel.2020.117523.

[3] Y. Li, F. Yang, X. Linxun, J. Liu, J. Wang, and X. Duan, "Influences of the control parameters and spark plug configurations on the performance of a natural gas spark-ignition engine," *Fuel*, vol. 324, p. 124728, 2022, doi: 10.1016/j.fuel.2022.124728.

[4] R. G. Papagiannakis, C. D. Rakopoulos, D. T. Hountalas, and D. C. Rakopoulos, "Emission characteristics of high speed, dual fuel, compression ignition engine operating in a wide range of natural gas/diesel fuel proportions," *Fuel*, vol. 89, no. 7, pp. 1397–1406, 2010, doi: 10.1016/j.fuel.2009.11.001.

[5] E. G. Giakoumis, "Diesel and spark ignition engines emissions and after-treatment control: Research and advancements," *Energies*, vol. 10, no. 11, pp. 3–6, 2017, doi: 10.3390/en10111882.

[6] N. Ghazaly and M. Salah Hofny, "Injection and Combustion of biodiesel at different blends: A review," *SVU-International Journal of Engineering Sciences and Applications*, vol. 3, no. 2, pp. 37–46, 2022, doi: 10.21608/svusrc.2022.130956.1043.

[7] F. Leach, G. Kalghatgi, R. Stone, and P. Miles, "The scope for improving the efficiency and environmental impact of internal combustion engines," *Transportation Engineering*, vol. 1, 2020, doi: 10.1016/j.treng.2020.100005.

[8] R. D. Reitz *et al.*, "IJER editorial: The future of the internal combustion engine," *International Journal of Engine Research*, vol. 21, no. 1, pp. 3–10, 2020, doi: 10.1177/1468087419877990.

[9] Z. Stępień, "A comprehensive overview of hydrogen-fueled internal combustion engines: Achievements and future challenges," *Energies*, vol. 14, no. 20, 2021, doi: 10.3390/en14206504.

[10] X. Zhen, Y. Wang, and D. Liu, "Bio-butanol as a new generation of clean alternative fuel for SI (spark ignition) and CI (compression ignition) engines," *Renewable Energy*, vol. 147, pp. 2494–2521, 2020, doi: 10.1016/j.renene.2019.10.119.

[11] V. Pandey, I. A. Badruddin, and T. M. Y. Khan, "Effect of H2 blends with compressed natural gas on emissions of SI engine having modified ignition timings," *Fuel*, vol. 321, p. 123930, 2022, doi: 10.1016/j.fuel.2022.123930.

[12] K. Chandrasekar, S. Sudhakar, R. Rajappan, S. Senthil, and P. Balu, "Present developments and the reach of alternative fuel: A review," *Materials Today: Proceedings*, vol. 51, pp. 74–83, 2021, doi: 10.1016/j.matpr.2021.04.505.

[13] D. Li *et al.*, "Study on combustion and emissions of a hydrous ethanol/gasoline dual fuel engine with combined injection," *Fuel*, vol. 309, p. 122004, 2022, doi: 10.1016/j.fuel.2021.122004.

[14] M. S. Hofny and N. M. Ghazaly, "A Review on Artificial Neural Network and Alternative Fuels for Internal Combustion Engines," *International Journal on Recent Technologies in Mechanical and Electrical Engineering*, vol. 9, no. 3, pp. 44–58, 2022.

[15] F. J. Joseph Shobana Bai, K. Shanmugaiah, A. Sonthalia, Y. Devarajan, and E. G. Varuvel, "Application of machine learning algorithms for predicting the engine characteristics of a wheat germ oil–Hydrogen fuelled dual fuel engine," *International Journal of Hydrogen Energy*, vol. 48, no. 60, pp. 23308–23322, 2023, doi: 10.1016/j.ijhydene.2022.11.101.

[16] Y. Zhang *et al.*, "The Prediction of Spark-Ignition Engine Performance and Emissions Based on the SVR Algorithm," *Processes*, vol. 10, no. 2, 2022, doi: 10.3390/pr10020312.

[17] M. A. Hassan, H. Salem, N. Bailek, and O. Kisi, "Random Forest Ensemble-Based Predictions of On-Road Vehicular Emissions and Fuel Consumption in Developing Urban Areas," *Sustainability (Switzerland)* , vol. 15, no. 2, pp. 1–22, 2023, doi: 10.3390/su15021503.

[18] X. Ding, C. Feng, P. Yu, K. Li, and X. Chen, "Gradient boosting decision tree in the prediction of NOx emission of waste incineration," *Energy*, vol. 264, 2023, doi: 10.1016/j.energy.2022.126174.

[19] M. A. Hashim, M. H. Nasef, A. E. Kabeel, and N. M. Ghazaly, "Combustion fault detection technique of spark ignition engine based on wavelet packet transform and artificial neural network," *Alexandria Engineering Journal*, vol. 59, no. 5, pp. 3687–3697, 2020, doi: 10.1016/j.aej.2020.06.023.

[20] T. Johnson and A. Joshi, "Review of Vehicle Engine Efficiency and Emissions," *SAE International Journal of Engines*, vol. 11, no. 6, pp. 1307–1330, 2018, doi: 10.4271/2018-01-0329.

[21] M. A. Hashim, M. H. Nasef, A. E. Kabeel, and N. M. Ghazaly, "Combustion fault detection technique of spark ignition engine based on wavelet packet transform and artificial neural network," *Alexandria Engineering Journal*, vol. 59, no. 5, pp. 3687–3697, 2020, doi: 10.1016/j.aej.2020.06.023.

[22] M. Munadi, M. Ariyanto, M. Muchammad, and J. D. Setiawan, "Optimal Engine Mapping Performances for Dual Spark-Plug Ignition Internal Combustion Engine Using Neural Network," *Journal of Applied Engineering Science*, vol. 20, no. 1, pp. 195–205, 2022, doi: 10.5937/jaes0-28542.

[23] G. J. Thompson, C. M. Atkinson, N. N. Clark, T. W. Long, and E. Hanzevack, "Technical Note: Neural network modelling of the emissions and performance of a heavy-duty diesel engine," *Proceedings of the Institution of Mechanical Engineers, Part D: Journal of Automobile Engineering*, vol. 214, no. 2, pp. 111–126, 2000, doi: 10.1177/095440700021400201.

[24] S. Bhowmik, R. Panua, S. K. Ghosh, A. Paul, and D. Debroy, "Prediction of performance and exhaust emissions of diesel engine fuelled with adulterated diesel: An artificial neural network assisted fuzzy-based topology optimization," *Energy and Environment*, vol. 29, no. 8, pp. 1413–1437, 2018, doi: 10.1177/0958305X18779576.

[25] H. Yaşar, G. Çağıl, O. Torkul, and M. Şişci, "Cylinder Pressure Prediction of An HCCI Engine Using Deep Learning," *Chinese Journal of Mechanical Engineering (English Edition)*, vol. 34, no. 1, 2021, doi: 10.1186/s10033-020-00525-4.

[26] N. Kuzhagaliyeva, A. Thabet, E. Singh, B. Ghanem, and S. M. Sarathy, "Using deep neural networks to diagnose engine pre-ignition," *Proceedings of the Combustion Institute*, vol. 38, no. 4, pp. 5915–5922, 2021, doi: 10.1016/j.proci.2020.10.001.

[27] A. Mat Deris, A. Mohd Zain, and R. Sallehuddin, "Overview of support vector machine in modeling machining performances," *Procedia Engineering*, vol. 24, pp. 308–312, 2011, doi: 10.1016/j.proeng.2011.11.2647.

[28] R. Fabrice and N. Villa, "Support vector machine for functional data classification," *Neurocomputing*, vol. 69, no. 7-9 SPEC. ISS., pp. 730–742, 2006, doi: 10.1016/j.neucom.2005.12.010.

[29] B. Liu, J. Hu, F. Yan, R. F. Turkson, and F. Lin, "A novel optimal support vector machine ensemble model for NOX emissions prediction of a diesel engine," *Measurement: Journal of the International Measurement Confederation*, vol. 92, no. 10, pp. 183–192, 2016, doi: 10.1016/j.measurement.2016.06.015.

[30] Y. Guo, Y. Liu, A. Oerlemans, S. Lao, S. Wu, and M. S. Lew, "Deep learning for visual understanding: A review," *Neurocomputing*, vol. 187, pp. 27–48, 2016, doi: 10.1016/j.neucom.2015.09.116.

[31] Y. Lecun, Y. Bengio, and G. Hinton, "Deep learning," *Nature*, vol. 521, no. 7553, pp. 436–444, 2015, doi: 10.1038/nature14539.

[32] S. Hussain, S. Gaftandzhieva, M. Maniruzzaman, R. Doneva, and Z. F. Muhsin, "Regression analysis of student academic performance using deep learning," *Education and Information Technologies*, vol. 26, no. 1, pp. 783–798, 2021, doi: 10.1007/s10639-020-10241-0.

[33] W. Ma *et al.*, "A deep convolutional neural network approach for predicting phenotypes from genotypes," *Planta*, vol. 248, no. 5, pp. 1307–1318, 2018, doi: 10.1007/s00425-018-2976-9.

[34] Z. B. Kizilkan, M. S. Sivri, I. Yazici, and O. F. Beyca, *Neural Networks and Deep Learning*. 2022. doi: 10.1007/978-3-030-93823-9_5.

[35] M. Azimi, A. D. Eslamlou, and G. Pekcan, *Data-driven structural health monitoring and damage detection through deep learning: State-ofthe- art review*, vol. 20, no. 10, 2020, doi: 10.3390/s20102778.

[36] S. Sengupta *et al.*, "A review of deep learning with special emphasis on architectures, applications and recent trends," *Knowledge-Based Systems*, vol. 194, p. 105596, 2020, doi: 10.1016/j.knosys.2020.105596.

[37] A. J. Astell *et al.*, "Using a touch screen computer to support relationships between people with dementia and caregivers," *Interacting with Computers*, vol. 22, no. 4, pp. 267–275, 2010, doi: 10.1016/j.intcom.2010.03.003.

[38] G. Nguyen *et al.*, "Machine Learning and Deep Learning frameworks and libraries for large-scale data mining: a survey," *Artificial Intelligence Review*, vol. 52, no. 1, pp. 77–124, 2019, doi: 10.1007/s10462-018-09679-z.

[39] S. Kabir, S. Patidar, X. Xia, Q. Liang, J. Neal, and G. Pender, "A deep convolutional neural network model for rapid prediction of fluvial flood inundation," *Journal of Hydrology*, vol. 590, 2020, doi: 10.1016/j.jhydrol.2020.125481.

[40] L. Eren, T. Ince, and S. Kiranyaz, "A Generic Intelligent Bearing Fault Diagnosis System Using Compact Adaptive 1D CNN Classifier," *Journal of Signal Processing Systems*, vol. 91, no. 2, pp. 179–189, 2019, doi: 10.1007/s11265-018-1378-3.

[41] J. Burner, L. Schwiedrzik, M. Krykunov, J. Luo, P. G. Boyd, and T. K. Woo, "High-performing deep learning regression models for

predicting low-pressure CO2 adsorption properties of metal−organic frameworks," *Journal of Physical Chemistry C*, vol. 124, no. 51, pp. 27996–28005, 2020, doi: 10.1021/acs.jpcc.0c06334.

[42] Ü. Ağbulut, A. E. Gürel, and S. Sarıdemir, "Experimental investigation and prediction of performance and emission responses of a CI engine fuelled with different metal-oxide based nanoparticles–diesel blends using different machine learning algorithms," *Energy*, vol. 215, 2021, doi: 10.1016/j.energy.2020.119076.

[43] S. Shin, S. Lee, M. Kim, J. Park, and K. Min, "Deep learning procedure for knock, performance and emission prediction at steady-state condition of a gasoline engine," *Proceedings of the Institution of Mechanical Engineers, Part D: Journal of Automobile Engineering*, vol. 234, no. 14, pp. 3347–3361, 2020, doi: 10.1177/0954407020932690.

[44] W. Lee, T. Y. Jung, and S. Lee, "Dynamic Characteristics Prediction Model for Diesel Engine Valve Train Design Parameters Based on Deep Learning," *Electronics (Switzerland)*, vol. 12, no. 8, 2023, doi: 10.3390/electronics12081806.

[45] L. Pulvirenti, L. Rolando, and F. Millo, "Energy management system optimization based on an LSTM deep learning model using vehicle speed prediction," *Transportation Engineering*, vol. 11, p. 100160, 2023, doi: 10.1016/j.treng.2023.100160.

[46] S. Cantero-Chinchilla, C. A. Simpson, A. Ballisat, A. J. Croxford, and P. D. Wilcox, "Convolutional neural networks for ultrasound corrosion profile time series regression," *NDT and E International*, vol. 133, p. 102756, 2023, doi: 10.1016/j.ndteint.2022.102756.

[47] Q. Dou, H. Luo, Z. Zhang, Y. Song, S. Chu, and Z. Mao, "A lightweight deep learning-based method for health diagnosis of internal combustion engines on an internet of vehicles platform," *Proceedings of the Institution of Mechanical Engineers, Part D: Journal of Automobile Engineering*, 2023, doi: 10.1177/09544070231198905.

[48] V. Vellandi, P. Namani, S. S. Bagavathy, and M. C. Mahindra, "Only Prevot for Distritio Pr for Distribution," pp. 1–5, 2020, doi: 10.4271/2023-01-0066.

[49] H. Tajima, T. Tomidokoro, and T. Yokomori, "Deep Learning for Knock Occurrence Prediction in SI Engines," *Energies*, vol. 15, no. 24, 2022, doi: 10.3390/en15249315.

[50] M. Rana, S. Sethuvenkatraman, R. Heidari, and S. Hands, "Solar thermal generation forecast via deep learning and application to buildings cooling system control," *Renewable Energy*, vol. 196, pp. 694–706, 2022, doi: 10.1016/j.renene.2022.07.005.

[51] J. Liao *et al.*, "A comparative investigation of advanced machine learning methods for predicting transient emission characteristic of diesel engine," *Fuel*, vol. 350, 2023, doi: 10.1016/j.fuel.2023.128767.

[52] W. He *et al.*, "Progress in prediction of remaining useful life of hydrogen fuel cells based on deep learning," *Renewable and Sustainable Energy Reviews*, vol. 192, p. 114193, 2024, doi: 10.1016/j.rser.2023.114193.

[53] J. F. Torres, D. Hadjout, A. Sebaa, F. Martínez-Álvarez, and A. Troncoso, "Deep Learning for Time Series Forecasting: A Survey," *Big Data*, vol. 9, no. 1, pp. 3–21, 2021, doi: 10.1089/big.2020.0159.

[54] A. N. Shmroukh and S. Ookawara, "Evaluation of transparent acrylic stepped solar still equipped with internal and external reflectors and copper fins," *Thermal Science and Engineering Progress*, vol. 18, p. 100518, 2020, doi: 10.1016/j.tsep.2020.100518.

[55] A. O. Hasan, H. Al-Rawashdeh, A. H. Al-Muhtaseb, A. Abu-jrai, R. Ahmad, and J. Zeaiter, "Impact of changing combustion chamber geometry on emissions, and combustion characteristics of a single cylinder SI (spark ignition) engine fueled with ethanol/gasoline blends," *Fuel*, vol. 231, pp. 197–203, 2018, doi: 10.1016/j.fuel.2018.05.045.

[56] A. O. Hasan, H. Al-Rawashdeh, A. Abu-jrai, M. R. Gomaa, and F. Jamil, "Impact of variable compression ratios on engine performance and unregulated HC emitted from a research single cylinder engine fueled with commercial gasoline," *International Journal of Hydrogen Energy*, vol. 48, no. 68, pp. 26619–26628, 2023, doi: 10.1016/j.ijhydene.2022.09.025.

[57] M. S. Hofny *et al.*, "Evaluation of ethanol-gasoline blends in SI engines using experimental and ANN techniques Evaluation of ethanol-gasoline blends in SI engines using experimental and ANN techniques," *Engineering Research Express*, vol. 6, 2024, doi: 10.1088/2631-8695/ad5f18.

[58] L. Zhong, L. Hu, and H. Zhou, "Deep learning based multi-temporal crop classification," *Remote Sensing of Environment*, vol. 221, pp. 430–443, 2019, doi: 10.1016/j.rse.2018.11.032.

[59] M. G. Ragab, S. J. Abdulkadir, and N. Aziz, "Random Search One Dimensional CNN for Human Activity Recognition," *2020 International Conference on Computational Intelligence, ICCI 2020*, pp. 86–91, 2020, doi: 10.1109/ICCI51257.2020.9247810.

[60] H. Gholamalinezhad and H. Khosravi, "Pooling Methods in Deep Neural Networks, a Review," *arXiv preprint arXiv:2009.07485*, 2020.

[61] C. C. Chen, Z. Liu, G. Yang, C. C. Wu, and Q. Ye, "An improved fault diagnosis using 1d-convolutional neural network model," *Electronics (Switzerland)*, vol. 10, no. 1, pp. 1–19, 2021, doi: 10.3390/electronics10010059.

[62] G. Wang, J. C. Ye, K. Mueller, and J. A. Fessler, "Image Reconstruction is a New Frontier of Machine Learning," *IEEE Transactions on Medical Imaging*, vol. 37, no. 6, pp. 1289–1296, 2018, doi: 10.1109/TMI.2018.2833635.

[63] Y. Yang, Q. M. J. Wu, X. Feng, and T. Akilan, "Recomputation of the dense layers for performance improvement of DCNN," *IEEE Transactions on Pattern Analysis and Machine Intelligence*, vol. 42, no. 11, pp. 2912–2925, 2020, doi: 10.1109/TPAMI.2019.2917685.

[64] M. Thoma, "Analysis and Optimization of Convolutional Neural Network Architectures," *arXiv preprint arXiv:1707.09725*, 2017.

[65] D. M. Pelt and J. A. Sethian, "A mixed-scale dense convolutional neural network for image analysis," *Proceedings of the National Academy of Sciences of the United States of America*, vol. 115, no. 2, pp. 254–259, 2017, doi: 10.1073/pnas.1715832114.

[66] S. Chauhan, M. Sharma, M. K. Arora, and N. K. Gupta, "Landslide susceptibility zonation through ratings derived from artificial neural network," *International Journal of Applied Earth Observation and Geoinformation*, vol. 12, no. 5, pp. 340–350, 2010, doi: 10.1016/j.jag.2010.04.006.

[67] S. Sharma, S. Sharma, and A. Athaiya, "Activation Functions in Neural Networks," *International Journal of Engineering Applied Sciences and Technology*, vol. 4, no. 12, pp. 310–316, 2020, doi: 10.33564/ijeast.2020.v04i12.054.

[68] M. L. Dering and C. S. Tucker, "A Convolutional Neural Network Model for Predicting a Product's Function, Given Its Form," *Journal of Mechanical Design*, vol. 139, no. 11, 2017, doi: 10.1115/1.4037309.

[69] Y.-S. Kim, M. K. Kim, N. Fu, J. Liu, J. Wang, and J. Srebric, "Investigating the Impact of Data Normalization Methods on Predicting Electricity Consumption in a Building Using different Artificial Neural Network Models.," *Sustainable Cities and Society*, p. 105570, 2024, doi: 10.1016/j.scs.2024.105570.

[70] Preeti, R. Bala, and R. P. Singh, "A dual-stage advanced deep learning algorithm for long-term and long-sequence prediction for multivariate financial time series," *Applied Soft Computing*, vol. 126, p. 109317, 2022, doi: 10.1016/j.asoc.2022.109317.

[71] X. Tang, H. Yao, Y. Sun, C. Aggarwal, P. Mitra, and S. Wang, "Joint modeling of local and global temporal dynamics for multivariate time series forecasting with missing values," *AAAI 2020 - 34th AAAI Conference on Artificial Intelligence*, pp. 5956–5963, 2020, doi: 10.1609/aaai.v34i04.6056.

[72] S. Marsi, J. Bhattacharya, R. Molina, and G. Ramponi, "A non-linear convolution network for image processing," *Electronics (Switzerland)*, vol. 10, no. 2, pp. 1–21, 2021, doi: 10.3390/electronics10020201.

[73] J. Wang, T. Jiang, Z. Cui, and Z. Cao, "Filter pruning with a feature map entropy importance criterion for convolution neural networks compressing," *Neurocomputing*, vol. 461, pp. 41–54, 2021, doi: 10.1016/j.neucom.2021.07.034.

[74] V. Varghese, M. Chikaraishi, and J. Urata, "Deep Learning in Transport Studies: A Meta-analysis on the Prediction Accuracy," *Journal of Big Data Analytics in Transportation*, vol. 2, no. 3, pp. 199–220, 2020, doi: 10.1007/s42421-020-00030-z.

[75] S. Zhang *et al.*, "An investigation of CNN models for differentiating malignant from benign lesions using small pathologically proven datasets," *Computerized Medical Imaging and Graphics*, vol. 77, p. 101645, 2019, doi: 10.1016/j.compmedimag.2019.101645.

[76] S. B. Navathe, W. Wu, S. Shekhar, X. Du, X. Sean Wang, and H. Xiong, "Database Systems for Advanced Applications: 21st International Conference, DASFAA 2016 Dallas, TX, USA, April 16–19, 2016 Proceedings, Part I," *Lecture Notes in Computer Science (including subseries Lecture Notes in Artificial Intelligence and Lecture Notes in Bioinformatics)*, vol. 9642, pp. 214–228, 2016, doi: 10.1007/978-3-319-32025-0.

[77] K. H. Ng, Y. S. Gan, C. K. Cheng, K. H. Liu, and S. T. Liong, "Integration of machine learning-based prediction for enhanced Model's generalization: Application in photocatalytic polishing of palm oil mill effluent (POME)," *Environmental Pollution*, vol. 267, p. 115500, 2020, doi: 10.1016/j.envpol.2020.115500.

[78] S. Mittal, "A Survey on optimized implementation of deep learning models on the NVIDIA Jetson platform," *Journal of Systems Architecture*, vol. 97, pp. 428–442, 2019, doi: 10.1016/j.sysarc.2019.01.011.

[79] D. Kilichev, D. Turimov, and W. Kim, "Next–Generation Intrusion Detection for IoT EVCS: Integrating CNN, LSTM, and GRU Models," *Mathematics*, vol. 12, no. 4, 2024, doi: 10.3390/math12040571.

[80] R. Maskeliūnas, A. Kulikajevas, R. Damaševičius, J. Griškevičius, and A. Adomavičienė, "Biomac3D: 2D-to-3D Human Pose Analysis Model for Tele-Rehabilitation Based on Pareto Optimized Deep-Learning Architecture," *Applied Sciences (Switzerland)*, vol. 13, no. 2, 2023, doi: 10.3390/app13021116.

[81] V. B. Sharma *et al.*, "Recent advancements in ai-enabled smart electronics packaging for structural health monitoring," *Metals*, vol. 11, no. 10, 2021, doi: 10.3390/met11101537.

[82] S. H. M. Rizvi and M. Abbas, "From data to insight, enhancing structural health monitoring using physics-informed machine learning and advanced data collection methods," *Engineering Research Express*, vol. 5, no. 3, 2023, doi: 10.1088/2631-8695/acefae.

[83] M. A. Hossain, R. K. Chakrabortty, S. Elsawah, and M. J. Ryan, "Very short-term forecasting of wind power generation using hybrid deep learning model," *Journal of Cleaner Production*, vol. 296, p. 126564, 2021, doi: 10.1016/j.jclepro.2021.126564.

[84] S. Srivastava, B. Paul, and D. Gupta, "Study of Word Embeddings for Enhanced Cyber Security Named Entity Recognition," *Procedia Computer Science*, vol. 218, pp. 449–460, 2022, doi: 10.1016/j.procs.2023.01.027.

[85] G. Alkhayat and R. Mehmood, "A review and taxonomy of wind and solar energy forecasting methods based on deep learning," *Energy and AI*, vol. 4, p. 100060, 2021, doi: 10.1016/j.egyai.2021.100060.

[86] Y. Wang, H. Zhang, and G. Zhang, "cPSO-CNN: An efficient PSO-based algorithm for fine-tuning hyper-parameters of convolutional neural networks," *Swarm and Evolutionary Computation*, vol. 49, pp. 114–123, 2019, doi: 10.1016/j.swevo.2019.06.002.

[87] E. Ayrey and D. J. Hayes, "The use of three-dimensional convolutional neural networks to interpret LiDAR for forest inventory," *Remote Sensing*, vol. 10, no. 4, pp. 1–16, 2018, doi: 10.3390/rs10040649.